Atmos. Chem. Phys., 8, 4855–4864, 2008
www.atmos-chem-phys.net/8/4855/2008/

Atmospheric Chemistry and Physics

Multiphase modeling of nitrate photochemistry in the quasi-liquid layer (QLL): implications for NO_X release from the Arctic and coastal Antarctic snowpack

C. S. Boxe and A. Saiz-Lopez

Earth and Space Science Div., NASA Jet Propulsion Laboratory, California Inst. of Technology, Pasadena, CA 91109, USA

Received: 18 January 2008 – Published in Atmos. Chem. Phys. Discuss.: 26 March 2008
Revised: 30 June 2008 – Accepted: 28 July 2008 – Published: 21 August 2008

Abstract. We utilize a multiphase model, CON-AIR (**Con**densed Phase to **Air** Transfer Model), to show that the photochemistry of nitrate (NO_3^-) in and on ice and snow surfaces, specifically the quasi-liquid layer (QLL), can account for NO_x volume fluxes, concentrations, and [NO]/[NO_2] (γ=[NO]/[NO_2]) measured just above the Arctic and coastal Antarctic snowpack. Maximum gas phase NO_x volume fluxes, concentrations and γ simulated for spring and summer range from 5.0×10^4 to 6.4×10^5 molecules cm^{-3} s^{-1}, 5.7×10^8 to 4.8×10^9 molecules cm^{-3}, and ~0.8 to 2.2, respectively, which are comparable to gas phase NO_x volume fluxes, concentrations and γ measured in the field. The model incorporates the appropriate actinic solar spectrum, thereby properly weighting the different rates of photolysis of NO_3^- and NO_2^-. This is important since the immediate precursor for NO, for example, NO_2^-, absorbs at wavelengths longer than nitrate itself. Finally, one-dimensional model simulations indicate that both gas phase boundary layer NO and NO_2 exhibit a negative concentration gradient as a function of height although [NO]/[NO_2] are approximately constant. This gradient is primarily attributed to gas phase reactions of NO_x with halogens oxides (i.e. as BrO and IO), HO_x, and hydrocarbons, such as CH_3O_2.

1 Introduction

Interest in the nitrogen cycle over the polar regions was revitalized due to elevated NO_x (NO+NO_2) levels detected in and above snowpacks (Honrath et al., 1999; Jones et al., 2000). Absorbing at $\lambda\geq290$ nm, nitrate (NO_3^-) is one of the dominant anions present in the snowpack with approximately an even surface distribution with latitude and longitude at both polar regions (Legrand and Meyeski, 1997; Mulvaney et al., 1998). Due to production and long-range transport, nitrate concentrations at the Arctic (~10 μM) are higher than those measured at coastal Antarctica (~5 μM). Through solar photolysis, nitrate is a major source of NO_x emissions from the snowpack. NO_x mixing ratios within and above the snowpack are proportional to NO_x production rates, time of day, and temperature (Cotter et al., 2003; Jones et al., 2000). Consequently, nitrate photochemistry has been the focus of a series of field (Honrath et al., 1999., 2000a, 2002; Jones et al., 2000; Davis et al., 2001, 2004; Zhou et al., 2001; Dibb et al., 2002, 2004; Qiu et al., 2002; Beine et al., 2002, 2003; Jacobi et al., 2004) and laboratory experiments (Honrath et al., 2000b; Dubowski et al., 2001, 2002; Chu and Anastasio, 2003, Boxe et al., 2003, 2005, 2006; Jacobi et al., 2006; Jacobi and Hilker, 2007).

If nitrate depth profiles in polar ice were preserved over time, they would provide a valuable record of global paleoatmospheres. However, physical and photochemical processing of nitrate can alter its surface and near-surface concentrations, especially at low-accumulation sites (Rothlisberger et al., 2002), and possibly compromise its isotopic signatures (Blunier et al., 2005; McCabe et al., 2005; Hastings et al., 2004). While the photochemistry of nitrate in the snowpack has significant implications for tropospheric chemistry, since its photoproducts, NO and NO_2, are intimately linked to reactions involving ozone, hydrocarbons and halogens, this process also generates OH radicals (see below), which can oxidize organic matter within snowpacks, leading to the

Correspondence to: C. S. Boxe
(christopher.boxe@jpl.nasa.gov)

formation of oxidized hydrocarbons (e.g. formaldehyde, acetaldehyde, acetone) (Dominé and Shepson, 1999; Sumner and Shepson, 2002; Grannas et al., 2004). In addition, HONO has been measured in the polar regions (Zhou et al., 2001; Honrath et al., 2002; Amoroso et al., 2006; Clemitshaw, 2006), where it has also been suggested as a possible byproduct of nitrate photolysis (Zhou et al., 2001). Yet, actual HONO concentrations and its source at polar sites have been debated (Chen et al., 2004; Dibb et al., 2004; Liao et al., 2006; Jacobi et al., 2007).

It is clear that overlying boundary layer chemistry is affected by photochemistry occurring at the snowpack at polar regions. A useful tool to study specified photochemical mechanisms occurring in the snowpack is to multiphase model boundary layer chemistry linked to chemistry at the snowpack surface, which requires a physicochemical understanding of ice surfaces. The ice-air interface of solids is an area that exhibits characteristics different from those of the bulk material. This is primarily due to the fact that atoms (or molecules) at the surface only encounter bonding forces with other molecules from one side; simultaneously, there is a similar imbalance at other interfaces. Furthermore, this behavior causes the dislocation of atoms from their original locations, alterations in their associated force and energy constants, and effects on layers below the ice-air demarcation. Michael Faraday in 1850 first suggested that the ice-air interface consists of a thin wet film (Faraday, 1850), variously called the quasi-liquid layer (QLL), premelting layer, liquid-like layer, or surface melting layer, by showing "that a particle of water which could retain the liquid state whilst touching ice on only one side, could not retain the liquid if it were touched by ice on both sides" (Faraday, 1850).

The fact that the boundary between the solid and vapor phase is wetted by a thin liquid film causes the free energy of the boundary to be lower than it would be if the thin liquid film were absent (Dash et al., 1995). As a result, if the surface of ice were initially dry, then it would reduce its interfacial free energy by converting a layer (e.g. the surface) of the solid to liquid. Hence, a liquid-like layer should exist over some measurable and quantifiable temperature range on the surface of ice, below its bulk normal melting temperature. The existence of the QLL is not prohibited due to its thinness and closeness to the normal melting temperature of ice and is present at a state where the free energy of the ice system is at a minimum and is governed by the competition between the free energy of the ice surface and the energy required to melt a solid layer.

The thickness of the QLL as a function of temperature has been quantified both experimentally (Doppenschmidt and Butt, 2000; Pittenger et al., 2001; Bluhm et al., 2002; Sadtchenko and Ewing, 2002) and theoretically (Ohnesorge et al., 1994; Landa et al., 1995; Wettlaufer, 1999). With the single exception of Elbaum et al. (1993), whose experiments were done on exposed horizontal facets in the prismatic orientation $10\bar{1}0$, these studies have shown that the QLL increases with increasing temperature. Additionally, impurities enhance its thickness (Doppenschmidt and Butt, 2000; Wettlaufer, 1999). The addition of impurities at constant pressure will shift the normal melting point of the bulk solid, which is directly dependent on the concentration of the impurity. As the melting point is approached, the QLL appears to be indistinguishable from the liquid phase in its uppermost layers. Concurrently, we do acknowledge that, at specified temperature regimes, below the actual melting point of pure water ice, the QLL is distinctly dissimilar than pure liquid water (e.g. its ability to take up trace gases). For instance, McNeill et al. (2006) showed for the first time that the solubility of HCl in the QLL, rather exhibiting a solubility similar that in a true-liquid matrix, exhibits a solubility that is intermediate between that in bulk ice and its respective solubility in a true-liquid matrix.

The QLL can play a pivotal role in environmental phenomena such as 1) controlling the friction of ice and snow; 2) soil freezing, permafrost formation, and frost heave; 3) sintering and sliding in glaciers, sea-ice, and snow fields; and 4) behavior of atmospheric ice (Dash et al., 1995). The QLL has also been suggested to contribute to the electrification of thunder clouds via charge transfer at the liquid-ice interface (Baker and Dash, 1994). Abbatt et al. (1992) and Molina (1994) even proposed that polar stratospheric clouds are able to accommodate HCl by dissolution in multilayer-thick quasi-liquid films, where they can efficiently participate in ozone destruction during winter and spring months in Antarctica and the Arctic. These hypotheses were later confirmed by seminal work, via laboratory analyses, showing explicitly that trace gases do efficiently accommodate snow/ice surfaces through trace-gas induce QLL formation McNeill et al. (2006).

As shown in Jones et al. (2007), spring and summertime maximum NO_x volume fluxes range from $\sim 4.5\times10^4$ to $\sim 5.5\times10^5$ molecules cm^{-3} s^{-1}. In addition, field measurements of NO_x range from $\sim 5.7\times10^8$ to $\sim 2.9\times10^9$ molecules cm^{-3} and exhibit $[NO]/[NO_2]$ (γ=$[NO]/[NO_2]$) from $\sim$0.8 to $\sim$2.0 (Honrath et al., 1999, 2002; Jones et al., 2000; Beine et al., 2002; Dibb et al., 2002; Simpson et al., 2007). In this study, we use CON-AIR to show that nitrate photochemistry in the QLL does simulate well NO_x volume fluxes, concentrations, and γ measured just above the snowpack (i.e. at $\sim$25 cm) at various sites in the Arctic and coastal Antarctica. The implications of these findings are also discussed.

2 Model description

CON-AIR is a multiphase model that treats the interaction of gas phase boundary layer chemistry with condensed phase chemistry and photochemistry in and on snow and ice surfaces, specifically the QLL. As described previously, here the QLL is defined as a thin layer on the surface of snow

and ice, where water molecules are not in a rigid solid structure, yet not in the random order of a liquid (Petrenko and Whitworth, 1999), which, in our model, is the demarcation between the vapor and bulk ice phase. It is structured in two main components: i) condensed phase chemistry and photochemistry regime in the QLL; and ii) gas phase chemistry scheme comprising photochemical, thermal, and heterogeneous reactions.

The exchange of nitrogen species between the QLL and the atmosphere depends on the respective Henry's law constants of species including NO and NO_2. The Henry's law solubility constants and temperature dependences for the gas phase equilibrating species NO and NO_2 are $1.9\times10^{-3}\times e^{(1500(1/T-1/To))}$ M atm^{-1} and $6.4\times10^{-3}e^{(2500(1/T-1/To))}$ M atm^{-1}, respectively (Schwartz and White, 1981; Lelieveld and Crutzen, 1991). The temperature dependence of the solubility of species is taken into account by including a diurnal variation of the typical temperature profile of both the Arctic and coastal Antarctic region during spring and summertime (i.e. 250≤T/K≤265). A description of the radiation and gas phase scheme, and a complete set of all gas phase reactions employed in the model are summarized in Table 1 of the supplementary material (http://www.atmos-chem-phys.net/8/4855/2008/acp-8-4855-2008-supplement.pdf).

2.1 Condensed phase scheme and QLL parameterizations

We note that the following formulation is developed within the context of a current overall shortage of physico-chemical data pertinent to the uptake and release of trace gases to snow/ice at conditions relevant for the polar snowpack. Bulk concentrations ofNO_3^- and NO_2^- (i.e. at the top few centimeters) at the Arctic and coastal Antarctic snowpack are $1\leq[NO_3^-]/\mu M\leq17$ and ∼1 nM, respectively (Stotlemyer and Toczydlowski, 1990; Jaffe and Zukowski, 1993; Li, 1993; Silvente and Legrand, 1995; De Angelis and Legrand, 1995; Dibb et al., 1998; Jones et al., 2007). A number of laboratory experiments have provided evidence that the photolysis of nitrate transpires in the QLL on the surface of ice crystals (Dubowski et al., 2001, 2002; Boxe et al., 2003; Chu and Anastasio, 2003). In this study, we restrict our model simulations within the context that all condensed phase reactions take place in the much smaller volume of the QLL. Typical bulk concentrations of NO_3^- and NO_2^- measured in the Arctic and coastal Antarctic snowpack were re-quantified following the formulation established by Cho et al. (2002). Cho et al. (2002) derived the following equation

$$\psi_{H_2O}(T) = \frac{m_{H_2O}\,RT_f}{1000H_f^0}\frac{T}{T_f-T}C_T^0, \quad (1)$$

which relates the fraction of liquid water (ψ_{H_2O}) as a function of temperature (T) and the total solute concentration in the QLL (C_T^0). $\psi_{H_2O}(T)$ is the fraction of water in the QLL as a function of temperature, m_{H_2O} is the molecular weight of water (18.01 g/mole), R is the gas constant (8.314×10^{-3} kJ/K mole), H_f^0 is enthalpy of fusion of water (6 kJ/mole), and T_f is the freezing temperature of water (273.15 K). Assuming that the total initial concentrations of NO_3^- and NO_2^- reside in the QLL, we relate their respective bulk concentrations (C_{bulk}) to their respective concentrations in the QLL via Eq. (2):

$$C_{bulk}=\psi_{H_2O}(T)C_T^0 \quad (2)$$

Substituting Eq. (1) into Eq. (2), yields the following:

$$\psi_{H_2O}(T) = \sqrt{\frac{m_{H_2O}\,RT_f}{1000H_f^0}\frac{T}{T_f-T}C_{bulk}}. \quad (3)$$

Then, given the upper limit $C_{bulk-upper-limit}$ (=17.0001 μM, $[NO_3^-]_o$=17 μM and $[NO_2^-]_o$=1 nM) and the lower limit $C_{bulk-lower-limit}$ (=1.0001 μM, $[NO_3^-]_o$=1 μM and $[NO_2^-]_o$=1 nM), we calculate 4.54×10^{-5} and 1.01×10^{-5} as the mean of the upper and lower limit ψ_{H_2O} from 250 to 265 K, respectively, by using Eqs. (4) and (5):

$$\text{mean of } \psi_{H_2O-upper-limit} = \frac{\sum_{i=250}^{i=265}\sqrt{\frac{m_{H_2O}\,RT_f}{1000H_f^0}\frac{T_i}{T_f-T_i}C_{bulk-upper-limit}}}{16}; \quad (4)$$

$$\text{mean of } \psi_{H_2O-lower-limit} = \frac{\sum_{i=250}^{i=265}\sqrt{\frac{m_{H_2O}\,RT_f}{1000H_f^0}\frac{T_i}{T_f-T_i}C_{bulk-lower-limit}}}{16}. \quad (5)$$

Summing the mean of $\psi_{H_2O-upper-limit}$ and themean of $\psi_{H_2O-lower-limit}$ gives 5.55×10^{-5}. In CON-AIR, as an approximation, we incorporate the average of this sum, 2.78×10^{-5}, as the fraction of liquid water, representative for temperatures from 250 to 265 K. Taking the mean of the median of $[NO_3^-]_o$ found both in the Arctic (i.e. from 3 to 17 μM) and coastal Antarctic (i.e. from 1 to 9 μM) yields 7.5 μM. Then, as an estimation, we take $[NO_3^-]_o$=7.5 μM and $[NO_2^-]_o$=1 nM as their initial bulk concentrations. Using Eq. (2), the concentration of $[NO_3^-]_o$ and $[NO_2^-]_o$ in the QLL is 270 mM and 0.04 mM, respectively, which we incorporate in CON-AIR as their initial concentrations.

Given our estimated $\psi_{H_2O}=2.78\times10^{-5}$, we calculate a QLL thickness ∼300 nm by the following formulation: snow depth × snow column cross-sectional area × mass fraction of liquid water = $1\,cm\times1\,cm^2\times2.78\times10^{-5}=2.78\times10^{-5}\,cm^3$; then, $2.78\times10^{-5}\,cm^3/1\,cm^2$=278 nm∼300 nm. This derived QLL thickness is comparable to previous laboratory measurements (Boxe, 2005; McNeill, 2005).

As an approximation, we use a use a conservative snow depth of 1 cm and a snow density of 0.31 g cm^{-3} (Michalowski et al., 2000; Sumner and Shepson, 1999). As a

Table 1. QLL reactions and rate constants.

Reactions	Aqueous rate constants[a]	QLL rate constants[b]
$NO_3^- + h\nu \rightarrow NO_2 + O^-$		[c]
$NO_3^- + h\nu \rightarrow NO_2^- + O(^3P)$		[c]
$NO_2^- + h\nu \rightarrow NO + O^-$		[d]
$O^- + H_2O \rightarrow {\cdot}OH + OH^-$	2.82×10^{-15} cm^3 molec^{-1} s^{-1}	2.82×10^{-15} cm^3 molec^{-1} s^{-1}/(volumetric)[e]
${\cdot}OH + OH^- \rightarrow O^- + H_2O$	2.00×10^{-11} cm^3 molec^{-1} s^{-1}	2.00×10^{-11} cm^3 molec^{-1} s^{-1}/(volumetric)[e]
$O_2 + O(^3P) \rightarrow O_3$	6.64×10^{-12} cm^3 molec^{-1} s^{-1}	6.64×10^{-12} cm^3 molec^{-1} s^{-1}/(volumetric)[e]
$O(^3P) + NO_2^- \rightarrow NO_3^-$	2.46×10^{-12} cm^3 molec^{-1} s^{-1}	2.46×10^{-12} cm^3 molec^{-1} s^{-1}/(volumetric)[e]
$O_3 + NO_2^- \rightarrow NO_3^- + O_2$	6.15×10^{-16} cm^3 molec^{-1} s^{-1}	6.15×10^{-16} cm^3 molec^{-1} s^{-1}/(volumetric)[e]
$NO_3^- + O(^3P) \rightarrow NO_2^- + O_2$	3.72×10^{-13} cm^3 molec^{-1} s^{-1}	3.72×10^{-13} cm^3 molec^{-1} s^{-1}/(volumetric)[e]
$NO_2^- + {\cdot}OH \rightarrow NO_2 + OH^-$	3.32×10^{-11} cm^3 molec^{-1} s^{-1}	3.32×10^{-11} cm^3 molec^{-1} s^{-1}/(volumetric)[e]
$NO_2 + NO_2 + H_2O \rightarrow NO_2^- + NO_3^- + 2H^+$	1.66×10^{-13} cm^3 molec^{-1} s^{-1}	1.66×10^{-13} cm^3 molec^{-1} s^{-1}/(volumetric)[e]
$NO + NO_2 + H_2O \rightarrow 2NO_2^- + 2H^+$	3.32×10^{-13} cm^3 molec^{-1} s^{-1}	3.32×10^{-13} cm^3 molec^{-1} s^{-1}/(volumetric)[e]
$NO + {\cdot}OH \rightarrow NO_2^- + H^+$	3.32×10^{-11} cm^3 molec^{-1} s^{-1}	3.32×10^{-11} cm^3 molec^{-1} s^{-1}/(volumetric)[e]
$NO_2 + {\cdot}OH \rightarrow NO_3^- + H^+$	2.16×10^{-12} cm^3 molec^{-1} s^{-1}	2.16×10^{-12} cm^3 molec^{-1} s^{-1}(volumetric)[e]
$NO + NO_2 \rightarrow N_2O_3$	1.83×10^{-12} cm^3 molec^{-1} s^{-1}	1.83×10^{-12} cm^3 molec^{-1} s^{-1}/(volumetric)[e]
$N_2O_3 + H_2O \rightarrow 2NO_2^- + 2H^+$	5.3×10^2 s^{-1}	5.3×10^2 s^{-1}
$2NO_2 \rightarrow N_2O_4$	7.48×10^{-13} cm^3 molec^{-1} s^{-1}	7.48×10^{-13} cm^3 molec^{-1} s^{-1}/(volumetric)[e]
$N_2O_4 + H_2O \rightarrow NO_2^- + NO_3^- + 2H^+$	10^3 s^{-1}	10^3 s^{-1}

[a] Aqueous phase reaction rate constants were obtained from Mack and Bolton (1999).
[b] QLL rate reaction rate constants were quantified by including the "volumetric" factor (Grannas et al., 2007; Takenaka et al., 1996).
[c] $J_{NO_3^-}$ values were extrapolated from Qui et al. (2002) and King et al. (2005).
[d] $J_{NO_2^-}$ was extrapolated from Zuo and Deng (1999).
[e] volumetric $\sim 8.20\times10^{-4}$ (Grannas et al., 2007; Takenaka et al., 1996).

result, the total potential liquid content in a snow column of 1 cm^2 cross-sectional area of snowpack is:

$$\text{total potential liquid content} = \frac{1\,\text{cm} \times 0.31\,\text{g cm}^{-3}}{1\,\text{g cm}^{-3}} = 0.31\,\text{cm}^3\,\text{cm}^{-2} \quad (6)$$

The estimated fraction of liquid water is 2.78×10^{-5}; therefore, the QLL volume at the snowpack surface:

$$\text{QLL volume} = 0.31\,\text{cm}^3\,\text{cm}^{-2} \times 2.78 \times 10^{-5} = 8.6 \times 10^{-6}\,\text{cm}^3\,\text{cm}^{-2} \quad (7)$$

To properly express aqueous phase reaction rates to QLL reaction rates, a volumetric factor (volumetric) was estimated based on laboratory derived reaction rate enhancement factors. A volumetric factor was quantified by taking the average of the upper limit reaction rate enhancement factors obtained in the laboratory by Grannas et al. (2007) and Takenaka et al. (1996), 40 and 2.4×10^3, respectively, yielding

$$\text{volumetric} = \frac{40 + 2.4 \times 10^3}{2} = 1.22 \times 10^3 \quad (8)$$

Therefore, the reaction rates are quantified by incorporating volumetric factor, volumetric. The rate constants for reactions taking place in the QLL are:

$$k \times \text{volumetric}, \quad (9)$$

$$k \times \text{volumetric}^2, \quad (10)$$

where k are the actual literature aqueous phase rate constants in units of cm^3 molecule^{-1} s^{-1} and cm^6 molecule^{-2} s^{-1}, for second- and third-order rate constants, respectively. Table 1 lists the major reactions pertaining to nitrate photochemistry, their condensed phase reaction rates, and their QLL reaction rates.

The rate constant for the transfer of species from the QLL to the gas phase is calculated using an approximation of the first order rate constant, $k_t = 1.25\times10^{-5}$ s^{-1} (Gong et al., 1997; Michalowski et al., 2000).

$$k_{\text{mix}} = k_t \times \frac{9.31 \times 10^{-6}\ \text{cm}^3\ \text{(QLL)}}{10,000\,\text{cm}^3\ \text{(atmosphere)}} \quad (11)$$

Nevertheless, the rate of transfer of species will depend on the concentration and Henry's law constants for solubility of the corresponding species. Hence, the complete expression

for the phase equilibration of species from the QLL to the atmosphere is:

$$k_{(\mathrm{QLL}\rightarrow\mathrm{Atmosphere})} = (k_{\mathrm{mix}} \times [\text{species concentration}] \times \text{volumetric}) / (H') , \quad (12)$$

where H' is the dimensionless Henry's law constant. H' is defined as $H'=(HRT)$, where H is a species' Henry's law constant, R is the gas constant, $0.082058\,\mathrm{L\,atm\,K^{-1}\,mol^{-1}}$, and T is the temperature (K).

3 Results and discussion

The photochemistry of nitrate in the aqueous phase has been studied extensively (Mark et al., 1996; Mack and Bolton, 1999). Dissolved nitrate has two primary absorption bands in the ultraviolet (UV). The first occurs in the far UV via the strong $\pi\rightarrow\pi^*$ transition, centered at 201 nm ($\varepsilon_{\max}$=9500 $\mathrm{M^{-1}\,cm^{-1}}$), and the second is a weaker absorption band that occurs via the highly forbidden $n\rightarrow\pi^*$ transition, centered at 302 nm ($\varepsilon_{\max}$=7.14 $\mathrm{M^{-1}\,cm^{-1}}$). Furthermore, it was proposed that the weaker absorption band may occur from the combination of a singlet and triplet $n\rightarrow\pi^*$ and $\sigma\rightarrow\pi^*$ transition (Maria et al., 1973).

Mack and Bolton (1999) showed that the overall stoichiometry for nitrate irradiation is

$$\mathrm{NO_3^-} \xrightarrow{h\nu} \mathrm{NO_2^-} + \frac{1}{2}\mathrm{O_2}. \quad (R1)$$

In the absence of $^{\cdot}$OH scavengers this stoichiometry is maintained over the entire pH range (Wagner and Strehlow, 1980). For λ<280 nm, the major reaction pathway is through isomerization of $[\mathrm{NO_3^-}]^*$, generated via Reaction (R2), to form $\mathrm{ONOO^-}$, peroxynitrite, and at low pH, peroxynitrous acid, HONOO (Reaction R3). HONOO can also be produced from the recombination of $^{\cdot}$OH and $\mathrm{NO_2}$ within a solvent cage as shown in Reaction (R4). HONOO isomerizes rapidly back to $\mathrm{NO_3^-}$ (Reaction R5) (Mack and Bolton, 1999).

$$\mathrm{NO_3^-} \xrightarrow{h\nu} [\mathrm{NO_3^-}]^* \quad (R2)$$

$$\mathrm{NO_3^-} \longrightarrow \mathrm{ONOO^-} + \mathrm{H^+} + \longrightarrow \mathrm{HONOO} \quad (R3)$$

$$^{\cdot}\mathrm{OH} + \mathrm{NO_2} \longrightarrow \mathrm{HONOO} \quad (R4)$$

$$\mathrm{HONOO} \longrightarrow \mathrm{NO_3^-} + \mathrm{H^+} \quad (R5)$$

Yet, in the troposphere, all λ<290 nm is completely attenuated by stratospheric ozone. Therefore, $\lambda\geq$290 nm are pertinent for this study. In aqueous solutions at pH<6 and $\lambda\geq$290 nm, nitrate photolysis proceeds via two primary photolytic pathways as illustrated in Reactions (R6) and (R7), through the generation of nitrate in the excited state, $[\mathrm{NO_3^-}]^*$, from Reaction (R2). As shown in Reaction (R8), $\mathrm{O^-}$ reacts rapidly with water to form the hydroxyl radical.

$$[\mathrm{NO_3^-}]^* + \mathrm{H^+} \longrightarrow \mathrm{NO_2} + \mathrm{O^-} \quad (R6)$$

$$[\mathrm{NO_3^-}]^* \longrightarrow \mathrm{NO_2^-} + \mathrm{O}(^3\mathrm{P}) \quad (R7)$$

$$\mathrm{O^-} + \mathrm{H_2O} \longrightarrow ^{\cdot}\mathrm{OH} + \mathrm{OH^-} \quad (R8)$$

Atomic oxygen produced in Reaction (R7) can react with molecular oxygen ($[\mathrm{O_2}]_{\mathrm{water}}\sim$0.3 mM) via Reaction (R9) or with nitrate by way of Reaction (R10) (Warneck and Wurzinger, 1988).

$$\mathrm{O_2} + \mathrm{O}(^3\mathrm{P}) \longrightarrow \mathrm{O_3} \quad (R9)$$

$$\mathrm{NO_3^-} + \mathrm{O}(^3\mathrm{P}) \longrightarrow \mathrm{NO_2^-} + \mathrm{O_2} \quad (R10)$$

Ozone, generated by Reaction (R9), is either consumed by reaction with $\mathrm{NO_2^-}$ (Reaction R11) (Hoigne et al., 1985) or by decomposition to $^{\cdot}$OH (Hoigne et al., 1985).

$$\mathrm{NO_2^-} + \mathrm{O_3} \longrightarrow \mathrm{NO_3^-} + \mathrm{O_2} \quad (R11)$$

The UV absorption spectrum of nitrite displays three absorption bands: the first involves a $\pi\rightarrow\pi^*$ transition with maxima at 220 nm, and the latter two peaks are maxima at 318 nm ($\varepsilon_{\max}$=10.90 $\mathrm{M^{-1}\,cm^{-1}}$) and 354 nm ($\varepsilon_{\max}$=22.90 $\mathrm{M^{-1}\,cm^{-1}}$), both corresponding to $n\rightarrow\pi^*$ transitions. Similar to nitrate, nitrite undergoes direct photolysis as shown in Reaction (R12) to produce NO, and it also oxidizes by reaction with $^{\cdot}$OH via Reaction (R13).

$$\mathrm{NO_2^-} + \mathrm{H^+} \xrightarrow{h\nu} \mathrm{NO} + ^{\cdot}\mathrm{OH} \quad (R12)$$

$$\mathrm{NO_2^-} + ^{\cdot}\mathrm{OH} \longrightarrow \mathrm{NO_2} + \mathrm{OH^-} \quad (R13)$$

The photolysis of $\mathrm{NO_2}$ also produces NO (Reaction R14). We exclude this reaction from the chemical scheme used in CON-AIR since its photolytic lifetime during midday spring and summertime ($1/J_{\mathrm{NO_2}}=1/4.6\times10^{-3}\,\mathrm{s^{-1}}\approx 217$ s) (Yung and DeMore, 1999) is longer than its diffusion lifetime through a $\sim$300 nm thick QLL (see above calculation). As calculated using the diffusion length equation (Eq. 13) (Dubowski et al., 2001):

$$\mathrm{NO_2} \xrightarrow{h\nu} \mathrm{NO} + \mathrm{O}(^3\mathrm{P}) \quad (R14)$$

$$L = \sqrt{D\tau};\ \tau = \frac{(300\times10^{-7}\,\mathrm{cm})^2}{9.8\times10^{-9}\,\mathrm{cm^2\,s^{-1}}} \approx 0.09\,\mathrm{s} \quad (13)$$

L is the thickness of the QLL, D is the diffusion coefficient of $\mathrm{NO_2}$ (Dubowski et al., 2001), and τ is the time it takes $\mathrm{NO_2}$ to diffuse through a thickness L. Using Eq. (13), we show that the maximum snowpack depth, starting from the top of the ice surface, where $\mathrm{NO_2}$ photolysis will not occur is $\approx(9.8\times10^{-9}\,\mathrm{cm^2\,s^{-1}}\times217\,\mathrm{s})^{1/2}\approx15\,\mu$m. Consequently, below 15 μm $\mathrm{NO_2}$ will undergo photolysis to produce NO, supporting the exclusion of this photolytic pathway. This estimation is further supported by previous findings, which have shown that $\mathrm{NO_2}$ produced from nitrate photolysis in the outermost layers of thin ice films are readily released to the gas phase, compared to $\mathrm{NO_2}$ formed at deeper depths,

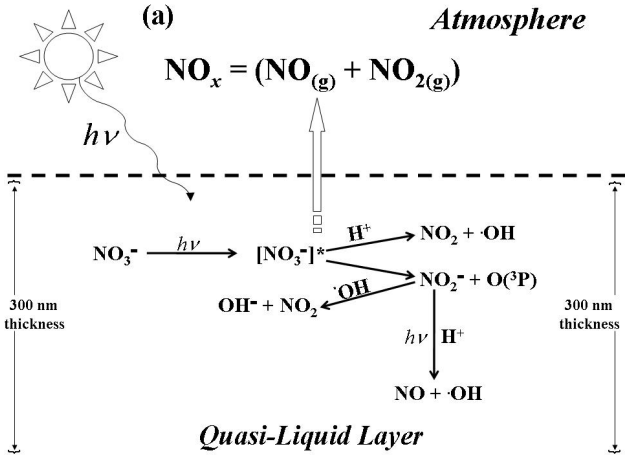

Fig. 1. Simplified schematic diagram illustrating the primary reactions governing NO_x release from a 300 nm thick QLL film to the gas phase from nitrate photochemistry. At QLL depths $<15\,\mu$m, NO_2 photolysis does not occur, while at QLL depths $>15\,\mu$m NO_2 photolysis occurs.

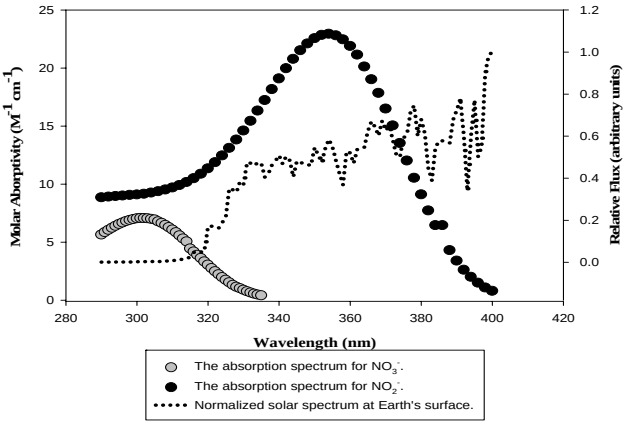

Fig. 2. The absorption spectrum for NO_3^- and NO_2^- (Gaffney et al., 1992; Zuo and Deng, 1998) and the normalized solar spectrum at the Earth's surface from 290 to 400 nm.

which undergoes further chemical and photolytic processing (Dubowski et al., 2001; Boxe et al., 2005, 2006). Finally, the photoproduced NO and NO_2 are readily released to the gas phase after equilibration due to their low solubility (Reaction R15).

$$NO_{2(QLL)},\ NO_{(QLL)} \xrightarrow{\text{escape}} NO_{2(g)},\ NO_{(g)} \qquad \text{(R15)}$$

The protonation of nitrite to form nitrous acid ($HONO_{(aq)}$) (Reaction R16) was also not considered in the QLL reaction mechanism since model simulations yielded $\gamma\sim1500$, much larger than any reported measurements from field studies (e.g. $\gamma\sim0.8$ to ~2.0) (Honrath et al., 1999, 2002; Jones et al., 2000, 2007; Beine et al., 2002; Dibb et al., 2002; Simpson et al., 2007). This result implies that a significant amount of HONO produced in the snowpack may be retained by matrix or solvent cage effects or may be dependent on photosensitized organic compounds, such as possible reaction cycles that may efficiently transfer electrons to NO_2, possibly leading to the production of HONO (Beine et al., 2006). Presently, the mechanism of HONO formation from NO_3^- is not well known.

$$NO_2^- + H^+ \longrightarrow HONO_{(aq)} \Leftrightarrow HONO_{(g)} \qquad \text{(R16)}$$

A simplified scheme illustrating the primary reactions governing NO_x release from the QLL film to the gas phase from nitrate photochemistry used in CON-AIR is shown in Fig. 1. Laboratory studies have shown that the photochemistry of nitrate in ice is analogous to its aqueous phase photochemistry (Dubowski et al., 2001, 2002; Chu and Anastasio et al., 2003; Boxe et al., 2006) Therefore, as shown in Table 1, QLL reaction rates were quantified by scaling aqueous phase reaction rates according to the micro-scopic dimensions of the QLL.

Laboratory studies have shown that nitrate is a source of NO and NO_2 from ice surfaces (Honrath et al., 2000b; Dubowski et al., 2001, 2002; Chu and Anastasio, 2003; Boxe et al., 2003, 2005, 2006; Jacobi et al., 2006; Jacobi and Hilker, 2007). Only a small number of laboratory investigations of nitrate photochemistry in ice were carried out to correlate their respective NO and NO_2 fluxes with field measurements (Boxe et al., 2003, 2006). Yet, these studies were restricted by high detection limits for NO and NO_2 and the use of irradiation sources emitting at 313 ± 20 nm (i.e. overlapping the absorption spectrum of nitrate), resulting in higher NO_x concentrations than measured in the field and much lower γ (e.g. 0.043 to 0.0005) than those measured over the Arctic and Antarctic snowpack (Boxe et al., 2003, 2006). Compared to the typical initial nitrate concentrations (1 to 20 μM) and the typical actinic flux spectrum at Earth's surface for the Arctic and coastal Antarctic regions, the higher initial nitrate concentrations (50 mM) and the dissimilar actinic flux spectrum used, likely contributed to the disparity between these laboratory results and those from the field. Figure 2 illustrates this disparity to some extent by comparing the absorption spectrum for nitrate and nitrite and the actinic flux spectrum at the Earth's surface. The surface irradiance is computed using a 2-stream radiative transfer code (Thompson, 1984). We calculate the diurnal variation of $J_{NO_3^-}$ and $J_{NO_2^-}$ for snowpack summer and springtime conditions by extrapolating laboratory modeled and measured $J_{NO_3^-}$ and $J_{NO_2^-}$ for ice, snowpack, and seawater (Zuo and Deng, 1998, Qiu et al., 2002; King et al., 2005) to the radiative transfer code, coupled to CON-AIR, such that $J_{NO_3^-}$ and $J_{NO_2^-}$ vary as a function of solar zenith angle (or as a function of time of day), therefore providing a more complete representation of nitrate photochemistry. Note, the smaller and larger summer/springtime diurnal profiles of $J_{NO_3^-}$ were derived from extrapolating

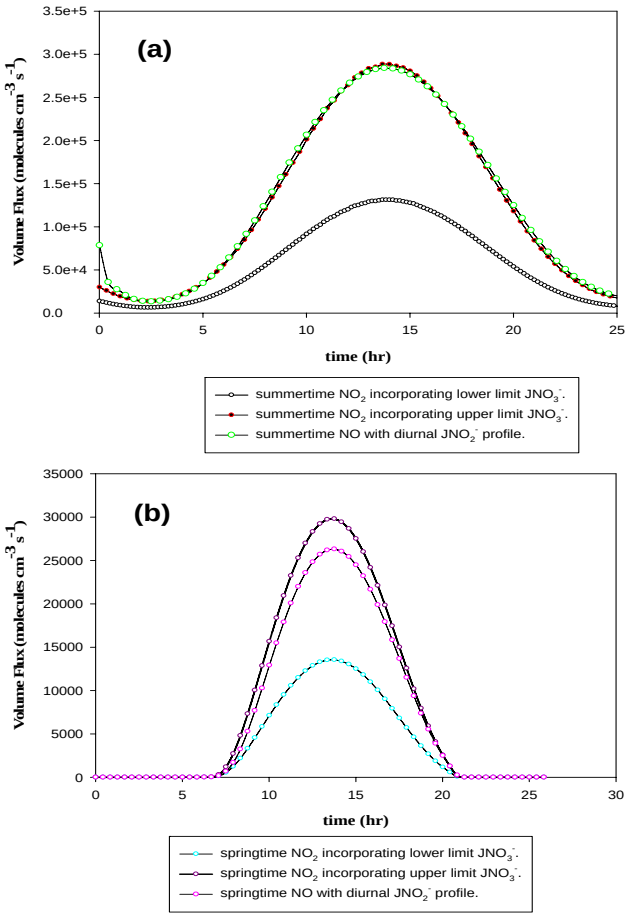

Fig. 3. **(a)** Simulated diurnal summer volume flux profiles of NO and NO_2 just above the snowpack. **(b)** Simulated diurnal springtime volume flux profiles of NO and NO_2 just above the snowpack.

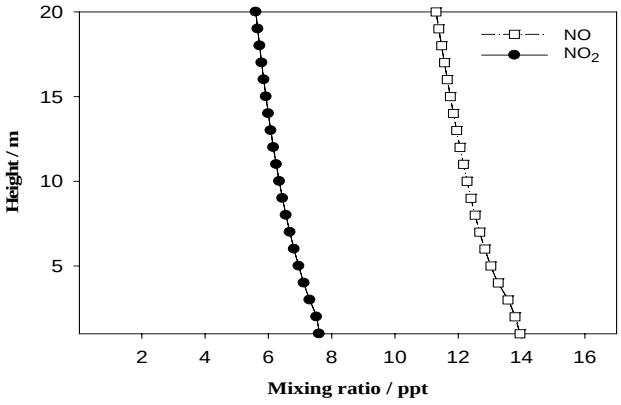

Fig. 4. Calculated summertime gas phase NO and NO_2 concentration profiles as a function of height above the snowpack.

the lower and upper limits for the $J_{NO_3^-}$ values obtained for surface snow and sea-ice (Qiu et al., 2002; King et al., 2005), while the summer/springtime diurnal profile of $J_{NO_2^-}$ was derived from extrapolating the $J_{NO_2^-}$ value obtained for surface seawater (Zuo and Deng, 1998). Figure 3 illustrates a typical diurnal profile for NO (e.g. maximum volume fluxes of 2.3×10^4 molecules cm^{-3} s^{-1} during spring and 3.2×10^5 molecules cm^{-3} s^{-1} during summer) and NO_2 (e.g. maximum concentrations of 1.2×10^4 molecules cm^{-3} s^{-1} to 2.7×10^4 molecules cm^{-3} s^{-1} during spring and 1.8×10^5 to 3.2×10^5 molecules cm^{-3} s^{-1} during summer) over the Arctic and Antarctic snowpack. These simulated NO_x volume fluxes are comparable to field measurements of Jones et al. (2007). Assuming a ~100 m boundary height and taking the median of the concentration of molecules between 250 and 265 K at atmospheric surface pressure (1 atm or 1.01325×10^5 N m^{-2}) (2.86×10^{19} molecules cm^{-3}), simulated maximum concentrations of NO_x, $\sim5.7\times10^8$ to $\sim4.8\times10^9$ molecules cm^{-3}, agree well with maximum concentrations of NO_x measured just above the snowpack by field measurements, $\sim5.7\times10^8$ to $\sim2.9\times10^9$ molecules cm^{-3}, (Honrath et al., 1999, 2002; Jones et al., 2000; Beine et al., 2002; Dibb et al., 2002; Simpson et al., 2007). It also accounts for the range of γ measured during Arctic and Antarctic summer and springtime, where springtime maximum γ ranges from ~0.84 to ~1.86 and summertime maximum γ ranges from ~0.50 to ~2.20, which is also in good accord with measured γ over the snowpack (Honrath et al., 1999, 2002; Jones et al., 2000; Beine et al., 2002; Dibb et al., 2002; Simpson et al., 2007). Furthermore, these model results reinforce laboratory and snow chamber results showing that the major source of NO release from snow/ice surfaces isNO_2^-, its immediate photolytic precursor that absorbs at wavelengths longer than nitrate itself (Cotter et al., 2003; Boxe et al., 2006), as shown in Fig. 2. Thus, incorporating the actinic flux at the Earth's surface shows that nitrite is more photolabile than nitrate (Cotter et al., 2003).

Furthermore, we investigate the profile of gas phase boundary layer NO and NO_2 as a function of height up to 20 m during the summertime over the snowpack using a 1-D model (Saiz-Lopez et al., 2008). Figure 4 shows that the model predicts a slight negative gradient for both [NO] and [NO_2], and γ remains approximately constant. The gradient is the result of gas phase reactions of NO_x with halogens oxides (i.e. BrO and IO), HO_x, and hydrocarbons (e.g. CH_3O_2) (Saiz-Lopez et al., 2008). Atmospheric stability and wind speed may also affect the concentration gradient of NO_x above the snowpack (Beine et al., 2002). However, constraining the 1-D model with the lower limit summertime NO and NO_2 volume fluxes derived from CON-AIR leads to good agreement with recent summertime observations of NO and NO_2 concentrations (13 ppt and 7 ppt as average noon values) and ratios ([NO]/[NO_2]~1.8) obtained at a few meters above the coastal Antarctic snowpack (e.g. Jones et al., 2007).

4 Summary and conclusions

We use a novel multiphase model, CON-AIR (**Con**densed Phase to **Air** Transfer Model) to show that the photochemistry of nitrate in and on snow/ice surfaces (i.e. the QLL) can account for measured NO and NO_2 volume fluxes, concentrations, and [NO]/[NO_2] measured just above the Artic and coastal Antarctic snowpack. Our model results produce comparable results although polar snowpack site physicochemical properties are dynamic and specific in nature. In addition, our model simulations suggest that, in general, nitrite photolysis (predominantly produced from nitrate photodecomposition) governs the release of NO_x just above the Arctic and coastal Antarctic snowpack, which is controlled by nitrite's coincident absorption spectrum with the solar spectrum at the polar snowpack surface. Finally, our model analyses show that NO and NO_2 display a negative concentration gradient as a function of height although their concentration ratios remain constant. We attribute this effect to gas phase reactions of these species with halogen oxides, HO_x, and hydrocarbons.

Acknowledgements. C. S. Boxe and A. Saiz-Lopez were supported by an appointment to the NASA Postdoctoral Program at the Jet Propulsion Laboratory, administered by Oak Ridge Associated Universities through a contract with the National Aeronautics and Space Administration (NASA). Research at the Jet Propulsion Laboratory, California Institute of Technology, under a contract with NASA, was supported by the NASA Upper Atmosphere Research and Tropospheric Chemistry Programs.

Edited by: V. F. McNeill

References

Amoroso, A., Beine, H. J., Sparapani, R., Nardino, M., and Allegrini, I.: Observations of coinciding arctic boundary layer ozone depletion and snow surface emissions of nitrous acid, Atmos. Environ., 40, 1949–1956, 2006.

Baker, M. B. and Dash, J. G.: Mechanism of change-transfer between colliding ice particles in thunderstorms, J. Geophys. Res.-Atmos., 99, 10 621–10 626, 1994.

Beine, H. J., Honrath, R. E., Dominé, F., Simpson, W. R., and Fuentes, J. D.: NO_xduring background and ozone depletion periods at Alert: fluxes above the snow surfaces, J. Geophys. Res., 107, 4584, doi:10.1029/2002JD002082, 2002.

Beine, H. J., Dominé, F., Ianniello, A., Nardion, M., Allegrini, I., Teinila, K., and Hillamo, R.: Fluxes of nitrate between snow surfaces and the atmosphere in the European high Arctic, Atmos. Chem. Phys., 3, 335–346, 2003, http://www.atmos-chem-phys.net/3/335/2003/.

Beine, H. J., Amoroso, A., Dominé, F., King, M. D., Nardino, M., Ianniello, A., and France, J. L.: Surprisingly small HONO emissions from snow surfaces at Browning Pass, Antarctica, Atmos. Chem. Phys., 6, 2569–2580, 2006, http://www.atmos-chem-phys.net/6/2569/2006/.

Bluhm, H., Olgetree, D. F., Fadley, C. S., Hussain, Z., and Salmeron, N.: The premelting of ice studied with photoelectron spectroscopy, J. Phys.-Condens. Matter, 14, L227–L233, 2002.

Blunier, T. G., Floch, L., Jacobi, H.-W., and Quansah, E.: Isotopic view on nitrate loss in Antarctic surface snow, Geophys. Res. Lett., 32, L13501, doi:10.1029/2005GL023011, 2005.

Boxe, C. S., Colussi, A. J., Hoffmann, M. R., Tan, D., Mastromarino, J., Case, A. T., Sandholm, S. T., and Davis, D. D.: Multiscale ice fluidity in NO_x photodesorption from frozen nitrate solutions, J. Phys. Chem. A, 107, 11 409–11 413, 2003.

Boxe, C. S.: Nitrate photochemistry and interrelated chemical phenomena in ice: influence of the quasi-liquid layer (QLL), Ph.D. thesis, California Institute of Technology, 2005.

Boxe, C. S., Colussi, A. J., Hoffmann, M. R., Murphy, J. G., Wooldridge, P. J., Betram, T. H., and Cohen, R. C.: Photochemical production and release of gaseous NO_2 from nitrate-doped water ice, J. Phys. Chem. A, 109, 8520–8525, 2005.

Boxe, C. S., Colussi, A. J., Hoffmann, M. R., Perez, I. M., Murphy, J. G., and Cohen, R. C.: Kinetics of NO and NO_2 evolution from illuminated frozen nitrate solutions, J. Phys. Chem. A, 110, 3578–3583, 2006.

Chen, G., Davis, D., Crawford, J., Hutterli, L. M., Huey, L. G., Slusher D., Mauldin, L., Eisele, F., Tanner, D., Dibb, J., Buhr, M., McConnell, J., Lefer, B., Shetter, r., Blake, D., Song, C. H., Lombardi, K., and Arnoldy, J.: A reassessment of HO_x South Pole chemistry based on observations recording during ISCAT 2000, Atmos. Environ., 38, 5451–5461, 2004.

Cho, H., Shepson, P. B., Barrie, L. A., Cowin, J. P., and Zaveri, R.: NMR investigations of the quasi-brine layer in ice/brine mixtures, J. Phys. Chem. B, 106, 11 226–11 232, 2002.

Chu, L. and Anastasio, C.: Quantum yields of hydroxyl radical and nitrogen dioxide from the photolysis of nitrate on ice, J. Phys. Chem. A, 107, 9594–9602 2003.

Clemitshaw, K. C.: Coupling between the tropospheric photochemistry of nitrous acid (HONO) and nitric acid (HNO_3), Environ. Chem., 3, 31–34, 2006.

Cotter, E. S. N., Jones, A. E., Wolff, E. W., and Baugitte, S. J.-B.: What controls photochemical NO and NO_2 production from Antarctic snow? Laboratory investigation assessing the wavelength and temperature dependence, J. Geophys. Res., 108, 4147, doi:10.1029/2002JD))2602, 2003.

Dash, J. G., Fu, H. Y., and Wettlaufer, J. S.: The premelting of ice and its environmental consequences, Rep. Prog. Physics, 58, 115–167, 1995.

Davis, D., Nowak, J. B., Chen, G., Buhr, M., Arimoto, R., Hogan, A., Eisele, F., Mauldin, L., Tanner, D., Shetter, R., Lefer, B., and McMurry, P.: Unexpected high levels of NO observed at South Pole, Geophys. Res. Lett., 28, 3625–3628, 2001.

Davis, D., Chen, G., Buhr, M., Crawford, J., Lenschow, D., Lefer, B., Shetter, R., Eisele, F., Mauldin, L., and Hogan, A.: South Pole NO_x chemistry: an assessment of factors controlling variability and absolute levels, Atmos. Environ., 38, 5375–5388, 2004.

De Angelis, D. and Legrand, M.: Preliminary investigations of postdepositional effects of HCl, HNO3, and organic acids in polar firn layers, in: Ice Core Studies of Global Biogeochemical Cycles, NATO ASI Ser., Ser. I, vol. 30, edited by: Delmas, R. J., Springer-Verlag, New York, 361–381, 1995.

Dibb, J. E., Arsenault, M., Peterson, M. C., and Honrath, R. E.:

Fast nitrogen oxide photochemistry in Summit, Greenland snow, Atmos. Environ., 36, 2501–2511, 2002.

Dibb, J. E., Huey, G. L., Slusher, D. L., and Tanner, D. J.: Soluble reactive nitrogen oxides at South Pole during ISCAT 2000, Atmos. Environ., 38, 5399–5409, 2004.

Dominé, F. and Shepson, P. B.: Air-snow interactions and atmospheric chemistry, Science, 297, 1506–1510, 2002.

Doppenschmidt, A. and Butt, H. J.: Measuring the thickness of the liquid-like layer on ice surfaces with atomic force microscopy, Langmuir, 16, 6709–6714, 2000.

Dubowski, Y., Colussi, A. J., and Hoffmann, M. R.: Nitrogen dioxide release in the 302 nm band photolysis of spray-frozen aqueous nitrate solutions. Atmospheric implications,J. Phys. Chem. A., 105, 4928-4932, 2001.

Dubowski, Y., Colussi, A. J., Boxe, C., and Hoffmann, M. R.: Monotonic increase of nitrite yields in the photolysis of nitrate in ice and water between 238 and 294 K, J. Phys. Chem., 106, 6967–6971, 2002.

Faraday, M.: Lecture before the Royal Institution reported in the Athaneum, 640, 1850.

Gaffney, J. S., Marley, N. A., and Cunningham, M. M.: Measurement of the absorption constants for nitrate in water between 270 and 335 nm, Environ. Sci. Technol., 25, 207–209, 1992.

Gong, S. L., Walmsley, J. L., Barrie, L. A., and Hopper, J. F.: Mechanisms for surface ozone depletion and recovery during Polar Sunrise, Atmos. Environ., 31(7), 969–981, 1997.

Grannas, A. M., Shepson, P. B., and Filley, T. R.: Photochemistry and nature of organic matter in Arctic and Antarctic snow, Global Biogeochem. Cycles, 18, GB1006, doi:10.1029/2003GB002133, 2004.

Hastings, M. G., Steig, E. J., and Sigman, D. M.: Seasonal variations in N and O isotopes of nitrate in snow at Summit, Greenland: Implications for the study of nitrate in snow and ice cores, J. Geophys. Res., 109, D20306, doi:10.1029/2004JD004991, 2004.

Hoigne, J., Bader, H., Haag, W. R., and Staehelin, J.: Rate constants of reactions with organic and inorganic compounds in water-III. Inorganic compounds and radicals, Water Res., 19, 993–1004, 1985.

Honrath, R. E., Peterson, M. C., Guo, S., Dibb, J. E., Shepson, P. B., and Campbell, B.: Evidence of NO_x production within or upon ice particles in the Greenland snowpack, Geophys. Res. Lett., 26, 695–698 1999.

Honrath, R. E., Peterson, M. C., Dziobak, M. P., Dibb, J. E., Arsenault, M. A., and Green, S. A.: Release of NO_x from sunlight-irradiated midlatitude snow, Geophys. Res. Lett., 26, 695–698, 2000a.

Honrath, R. E., Guo, S., Peterson, M. C., Dziobak, M. P., Dibb, J. E., and Arsenault, M. A.: Photochemical production of gas phase NO_x from ice crystal NO_3^-, J. Geophys. Res., 105, 24 183–24 190, 2000b.

Honrath, R. E., Lu, Y., Peterson, M. C., Dibb, J. E., Arsenault, M. A., Cullen, N. J., and. Steffen, K.: Vertical fluxes of NO_x, HONO, and HNO_3 above the snowpack at Summit, Greenland, Atmos. Environ., 36, 2629–2640, 2002.

Jacobi, H.-W., Bales, R. C., Honrath, R. E., Peterson, M. C., Dibb, J. E., Swanson, A. L., and Albert, M. R.: Reactive trace gases measured in the interstitial air of surface snow at Summit, Greenland, Atmos. Environ., 38, 1687–1697, 2004.

Jacobi, H.-W., Annor, T., and Quansah, E.: Investigation of the photochemical decomposition of nitrate, hydrogen peroxide, and formaldehyde in artificial snow, J. Photochem. Photobiol. A., 179, 330–338, 2006.

Jacobi, H.-W. and Hilker, B.: A mechanism for the photochemical transformation of nitrate in snow, J. Photochem. Photobiol. A, 185, 371–382, 2007.

Jaffe, D. A. and Zukowski, M. D.: Nitrate deposition to the Alaska snowpack, Atmos. Environ., 27A, 2935–2941, 1993.

Jones, A. E., Weller, R., Wolff, E. W., and Jacobi, H.-W.: Speciation and rate of photochemical NO and NO_2 production from Antarctic snow, Geophys. Res. Lett., 27, 345–348, 2000.

Jones, A. E., Wolff, E. W., Ames, D., Bauguitte, S. J.-B., Clemitshaw, K. C., Fleming, Z., Mills, G. P., Saiz-Lopez, A., Salmon, R. A., Sturges, W. T., and Worton, D. R.: The multi-seasonal NOy budget in coastal Antarctica and its link with surface snow and ice core nitrate: results from the CHABLIS campaign, Atmos. Chem. Phys. Discuss., 7, 4127–4163, 2007, http://www.atmos-chem-phys-discuss.net/7/4127/2007/.

King, M. D., France, J. L., Fisher, F. N., and Beine, H. J.: Measurement and modeling of UV radiation penetration and photolysis rates of nitrate and hydrogen peroxide in Antarctic sea ice: An estimate of the production rate of hydroxyl radicals in first-year sea ice, J. Photochem. Photobiol. A, 176, 39–49, 2005.

Legrand, M. and Mayewski, P.: Glaciochemistry of polar ice cores: a review, Rev. Geophys., 35, 219–243, 1997.

Landa, A., Wynblatt, P., Hakkinen, H., Barnett, R. N., and Landman, U.: Equilibrium interphase interfaces and premelting of the Pb(110) surface, Phys. Rev. B, 51, 10 972–10 980, 1995.

Lelieveld, J. and Crutzen, P. J.: The role of clouds in tropospheric photochemistry, J. Atmos. Chem., 12, 229–267, 1991.

Li, S.-M.: Particulate and snow nitrite in the spring arctic troposphere, Atmos. Environ., 27, 2959–2967, 1993.

Liao, W., Case, A. T., Mastromarino, J., Tan, D., and Dibb, J. E.: Observations of HONO by laser-induced fluorescence at the Sout Pole during ANTCI 2003, Geophys. Res. Lett., 33, L09810, doi:10.1029/2005GL025470, 2006.

Mack, J. and Bolton, J. R.: Photochemistry of nitrite and nitrate in aqueous solution: a review, J. Photochem. Photobiol. A, 128, 1–13, 1999.

Maria, H. J., McDonald, J. R., and McGlynn, S. P.: Electronic absorption spectrum of nitrate ion and boron trihalides, J. Am. Chem. Soc., 95, 1050–1056, 1973.

Mark, G., Korth, H.-G., Schuchmann, H.-P., and von Sonntag, C.: The photochemistry of aqueous nitrate ion revisited, J. Photochem. Photobiol. A, 101, 89–103, 1996.

McCabe, J. R., Boxe, C. S., Colussi, A. J., Hoffmann, M. R., and Thiemens, M. H.: Oxygen isotopic fractionation in the photochemistry of nitrate in water and ice, J. Geophys. Res., 110, D15310, doi:10.1029/2004JD005484, 2005.

McNeill, V. F.: Studies of Heterogeneous Ice Chemistry Relevant to the Atmosphere, Ph.D. thesis, Massachusetts Institute of Technology, 2005.

McNeill, V. F., Loerting, T., Geiger, F. M., Trout, B. L., and Molina, M. J.: Hydrogen chloride-induced surface disordering on ice, Proc. Natl. Acad. Sci. USA, 103, 9422–9427, 2006.

Michalowski, B. A., Francisco, J. S., Li, S.-M., Barrie, L. A., Bottenheim, J. W., and Shepson, P. B.: A computer model study of multiphase chemistry in the Arctic boundary layer during polar

sunrise, J. Geophys. Res., 105, 15 131–15 145, 2000.

Molina, M. J.: The Probable Role of Stratospheric 'Ice' Clouds: Hetergeneous Chemistry of the 'Ozone Hole', in: The Chemistry of the Atmosphere: The Impact of Global Change, edited by: Calvert, J. G., pp. 27–38, Blackwell Scientific Publications, Boston, 1994.

Mulvaney, R., Wagenback, D., and Wolff, E. W.: Postdepositional change in snowpack nitrate from observation of year-round near-surface snow in coastal Antarctica, J. Geophys. Res., 103, 11 021–11 031, 1998.

Ohnesorge, R., Lowen, H., and Wagner, H.: Density-Functional theory of crystal fluid interfaces and surface melting, Phys. Rev. E, 50, 4801–4809, 1994.

Petrenko, V. F. and Whitworth, R. W.: Physics of Ice, Oxford University Press, New York, 1999.

Pittenger, B., Fain, S. C., Cochran, M. J., Donev, J. M. K., Robertson, B. E., Szuchmacher, A., and Overney, R. M.: Premelting at ice-solid interfaces studied via velocity-dependent indentation with force microscope tips, Phys. Rev. B, 63, 134 102, 2001.

Qiu, R., Green, S. A., Honrath, R. E., Peterson, M. C., Lu, Y., and Dziobak, M.: Measurements of $J_{NO_3^-}$ in snow by nitrate-based actinometry, Atmos. Environ., 36, 2563–2571, 2002.

Rothlisberger, R., Hutterli, M. A., Wolff, E. W., Mulvaney, R., Fischer, H., Bigler, M., Goto-Azuma, K., Hansson, M. E., Ruth, U., Siggaard-Andersen, M. L., and Steffensen, J. P.: Nitrate in Greenland and Antarctic ice cores: a detailed description of post-depositional processes, Ann. Glaciol., 35, 209–216, 2002.

Sadtchenko, V. and Ewing, G. E.: Interfacial melting of thin ice films: An infrared study, J. Chem. Phys., 116, 4686–4697, 2002.

Saiz-Lopez, A., Plane, J. M. C., Mahajan, A. S., Anderson, P. S., Bauguitte, S. J.-B., Jones, A. E., Roscoe, H. K., Salmon, R. A., Bloss, W. J., Lee, J. D., and Heard, D. E.: On the vertical distribution of boundary layer halogens over coastal Antarctica: implications for O_3, HO_x, NO_x, and the Hg lifetime, Atmos. Chem. Phys., 8, 887–900, 2008, http://www.atmos-chem-phys.net/8/887/2008/.

Schwartz, S. E. and White, W. H.: Solubility equilibria of the nitrogen oxides and oxyacids in dilute aqueous solution, in: Advances in Environmental Science and Engineering, edited by: Pfafflin, J. R. and Ziegler, E. N., 4, 1–45, 1981.

Silvente, E. and Legrand, M.: A preliminary study of air-snow relationship for nitric acid in Greenland, in: Ice Core Studies of Global Biogeochemical Cycles, NATO ASI Ser., Ser. I, vol. 30, edited by: Delmas, R. J., Springer-Verlag, New York, 225–240, 1995.

Simpson, W. R., von Glasow, R., Riedel, K., Anderson, P., Bottenheim, J., Burrows, J., Carpenter, L. J., Frieß, Goodsite, M. E., Heard, D., Hutterli, M., Jacobi, H.-W., Kaleschke, L., Neff, B., Plane, J., Platt, U., Richter, A., Roscoe, H., Sander, R., Shepson, P., Sodeau, J., Steffen, A., Wagner T., and Wolff, E.: Halogens and their role in polar boundary-layer ozone depletion, Atmos. Chem. Phys., 7, 4375–4418, 2007, http://www.atmos-chem-phys.net/7/4375/2007/.

Stottlemeyer, R. and Toczydlowski, D.: Pattern of solute movement from snow into an Upper Michigan stream, Can. J. Fish. Aquat. Sci., 47, 290–300, 1990.

Sumner, A. L. and Shepson, P. B.: Snowpack production of formaldehyde and its effect on the Arctic troposphere, Nature, 398, 230–233, 1999.

Thompson, A. M.: The effects of clouds on photolysis rates and ozone formation in the unpolluted troposphere, J. Geophys. Res.-Atmos., 89, 1341–1349, 1984.

Wagner, I. and Strehlow, H. Z.: Flash photolysis of nitrate ions in aqueous solutions, Phys. Chemie. Neue Folge, 123, 1–33, 1980.

Warneck, P. and Wurzinger, C.: Product quantum yields for the 305-nm photodecomposition of NO_3^- in aqueous solution, J. Phys. Chem., 92, 6278–6283, 1988.

Wettlaufer, J. S.: Impurity effects in the premelting of ice, Phys. Rev. Lett., 82, 2516–2519, 1999.

Yung, Y. L. and Demore, W. B.: Photochemistry of Planetary Atmospheres, Oxford University Press, 1999.

Zhou, X., Beine, H. J., Honrath, R. E., Fuentes, J. D., Simpson, W., Shepson, P. B., and Bottenheim, J. W.: Snowpack photochemical production of HONO: a major source of OH in the arctic boundary layer in springtime, Geophys. Res. Lett., 28, 4087–4090, 2001.

Zuo, Y. and Deng, Y.: The near-UV absorption constants for nitrite ion in aqueous solution, Chemosphere, 36, 181–188, 1998.